Journal of
Applied Remote Sensing

Characterization, testing, calibration, and validation of the Berlin emissivity database

Alessandro Maturilli
Joern Helbert

SPIE

Characterization, testing, calibration, and validation of the Berlin emissivity database

Alessandro Maturilli* **and Joern Helbert**
German Aerospace Centre, Institute for Planetary Research, Rutherfordstrasse 2, Berlin, 12489, Germany

Abstract. The Berlin emissivity database is a spectral library providing a basis for the interpretation of thermal emission spectra of planetary regoliths. It contains spectra of plagioclase and potassium feldspars, low and high Ca pyroxenes, olivine, sulfur, Martian analogs, and a lunar highland sample in the wavelength range 3–50 μm. Four particle sizes with dimensions <25, 25–63, 63–125, 125–250 μm are measured for each sample. An exhaustive suite of tests was implemented, to characterize the setup in the planetary emissivity laboratory and the emissivities collected in the spectral library. The tests improve the quality of measurements, optimizing the sample preparation, calibration algorithm, sample, blackbody, and chamber temperatures, and all the parameters entering in the measurements or calibration processes. The results of our tests are shown and discussed, together with the implications that these results have on the development of the measurement and calibration procedures. [DOI: 10.1117/1.JRS.8.084985]

Keywords: experimental techniques; mineralogy; spectroscopy.

Paper 13497SS received Nov. 30, 2013; revised manuscript received Apr. 15, 2014; accepted for publication Apr. 17, 2014; published online May 19, 2014.

1 Introduction

In the last several decades, vibrational spectroscopy has been frequently used in the thermal infrared (TIR) region to determine the composition of organic and inorganic materials. The fundamental principle of this research area is that in a crystal lattice, vibrational motions occur at some particular frequencies, associated with the crystal structure and elemental composition.[1,2] For most of the rock-forming minerals, fundamental vibrations of atoms in the crystal lattice take place in the 5- to 50-μm region of the TIR,[3] while for some minerals, overtones and combinations can produce absorptions at shorter wavelengths.[4]

Numerous previous works investigated the thermal IR spectrum,[1,5] and demonstrated that the vibrational motions of atoms or ions within a mineral crystal originate spectral bands of which variability in the IR spectral region is strongly correlated to mineral composition, crystal structure, particle size, and observing geometry.[3]

Thermal emission spectroscopy, among the different available techniques to perform such analysis, is the method of data acquisition most similar to remotely sensed data in the TIR spectral range, allowing for a direct, quantitative comparison between laboratory and remote sensing instruments data sets.[6] To build the Berlin emissivity database (BED) spectral library, we followed the method developed in Ref. 7 and successively revised by Ref. 8, and the methodologies described in Refs. 6 and 8.

This paper illustrates an exhaustive set of test measurements that have been performed to study and characterize the stability of our measurements, instrumental error, error in the sample preparation, error induced by the instrument operator, to characterize some hardware components of our system (e.g., the external windows and the emissivity chamber), to quantify the improvement on the data quality when using an evacuated instrument, and to improve the

*Address all correspondence to: Alessandro Maturilli, E-mail: alessandro.maturilli@dlr.de

data calibration process in its various aspects. The device used is coupled to a Fourier-transform infrared (FTIR) Bruker VERTEX80v, working under vacuum. The spectral interval 3–16 μm is covered using an mercury cadmium telluride (MCT) cooled detector, for the 16- to 50-μm spectral range, a room temperature deuterated triglycine sulphate (DTGS) detector is used. Spectra are acquired with a spectral resolution of at least 2 cm^{-1}.

To decrease the time of data acquisition, most of the tests have been realized with the instrument in the MCT detector setup alone, and only these data will be discussed in the paper. For the DTGS configuration, only tests on repeatability were performed; we show those results at the end of the paper.

2 Sample Preparation and Apparatus

The BED spectral library contains spectra of planetary analog materials, separated in four grain size ranges: <25, 25–63, 63–125, and 125–250 μm.

The minerals, after being fragmented and ground, are wet- or dry-sieved, to get the standard size fractions, and then placed into aluminum cups, with 5-cm internal diameter and depth varying from 1.5 to 5 mm (depending on the amount of the available material), and then placed in an oven at 155°C for several hours, to reduce the content of adsorbed water and to reach the measuring temperature.

The spectral measurements are performed with a FTIR spectrometer Bruker VERTEX 80v, working under vacuum (~0.8 mbar). To cover the 3- to 16-μm spectral range, a liquid nitrogen cooled mercury-cadmium-telluride detector, a potassium-bromide (KBr) beamsplitter, and a KBr entrance port are used. The 16- to 50-μm spectral range is measured using a room temperature DTGS detector, a Mylar multilayer beamsplitter, and a caesium-iodide (CsI) entrance port.

The emissivity device consists of the sample chamber, a double-walled box with three apertures: a 15-cm squared door used to insert the cup in the chamber, a 5-cm rounded opening through which the beam is directed to the spectrometer, and a 5-cm opening facing the attached blackbody unit. A heater is installed in the chamber and is used to heat the cup with the samples from the bottom. The thermal radiation emitted normal to the surface by the sample or the blackbody is collected by a moving Au-coated parabolic off-axis mirror and reflected to the entrance port of the spectrometer.

A pump circulates water at a constant temperature (20°C) in the volume between the inner and outer walls of the chamber. The surfaces of the box are painted with black high-emissivity paint. The chamber is purged with dry air to remove particulates, water vapor, and CO_2. Further details can be found in Refs. 6 and 8.

3 Calibration of the Measurements

The data calibration procedure has been described in Ref. 8 and has remained the same over the years. Nevertheless, some tests have been carried out to identify potential improvements in the procedure.

Two blackbody measurements are taken at the beginning of every session, to determine the response function, following the equation[8]

$$F = \frac{I_{BB}(T_1) - I_{BB}(T_2)}{B_{BB}(T_1) - B_{BB}(T_2)}, \tag{1}$$

where I_{BB} are the raw measurements for two temperatures of the blackbody (T_1 and T_2), and B_{BB} are the Planck functions calculated for the same temperatures. Differentiating the blackbody measurements at two temperatures should remove or at least minimize any contribution from the spectrometer or the environment to the data. However, we are aware that self-emitted light from the FTIR contributes to the measured signal, but contains a phase error different from that of the sample and blackbody sources;[9] hence we may not eliminate all of the phase errors properly.

We examined several pairs of temperatures to find the best definition of the response function [F in Eq. (1)]. Figure 1 shows the three calculated F from measured blackbodies at 40°C, 100°C, and 175°C. The F for the three pairs of temperatures (upper panel and lower left) is shown,

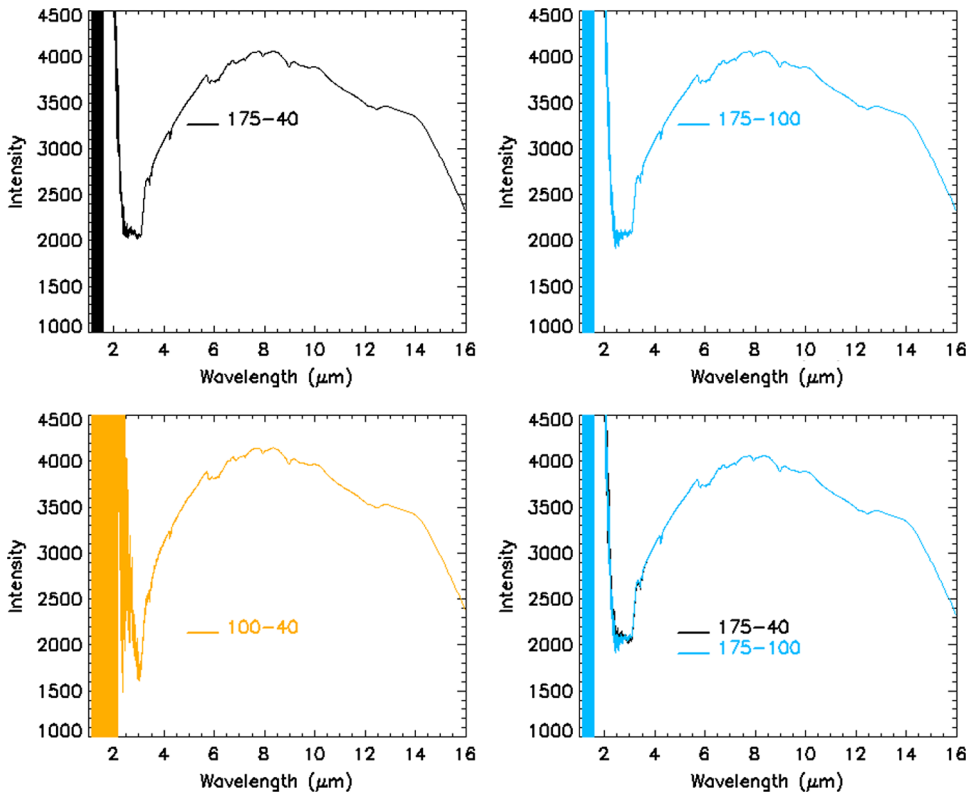

Fig. 1 Instrument response function (F) calculated for three couples of blackbody temperatures (upper and lower-left panels), and the comparison between the two best cases.

together with a comparison between the two best candidates. Though we got very good results for all the four couples, we decided to chose the F obtained with the highest available temperature (175°C) coupled with the lowest possible temperature (40°C), because it gives a better signal-to-noise ratio (SNR) for wavelength shorter than 4 μm, a spectral range that even if outside the performance study reported in this paper, we aim to cover at best.

Instrument energy ($\varepsilon_{\text{inst}}B_{\text{inst}}$) takes into account of all the energy that reaches the detector not originating from the sample. This contribution is determined using a blackbody measurement and the response function determined from Eq. (1)[8]

$$\varepsilon_{\text{inst}}B_{\text{inst}} = B_{\text{BB}} - \frac{I_{\text{BB}}}{F}. \tag{2}$$

An improvement in the calibration procedure and therefore in the data quality was achieved, by considering our blackbody not as ideal (emissivity equals 1.0 along the whole wavelengths range), but real, following the emissivity curve obtained from the manufacturer. Its real emissivity varies between 0.95 and 0.97, and in Fig. 2 is shown how the calibrated data for a sample of quartz in the grain size range of 125–250 μm changes when introducing this refinement. The black curve is the emissivity calculated when treating our blackbody as real, which it is using its real emissivity curve, the blue one is for the same sample calibrated assuming an ideal blackbody (emissivity equal 1.0).

Note how distorted the curve is for the "Ideal BB" case in comparison with the "real BB" emissivity: the data are tilted around the Reststrahlen band of quartz, the typical "doublet" in the region between 8 and 10 μm. This tilting has the effect of shifting the emissivity maximum for the "Ideal BB" case to wavelength larger than 12 μm. This is completely unrealistic, since the maximum in emissivity [also known as Christensen feature, (CF)] for quartz has a well-known position around the 7.4 μm.[3,7,10]

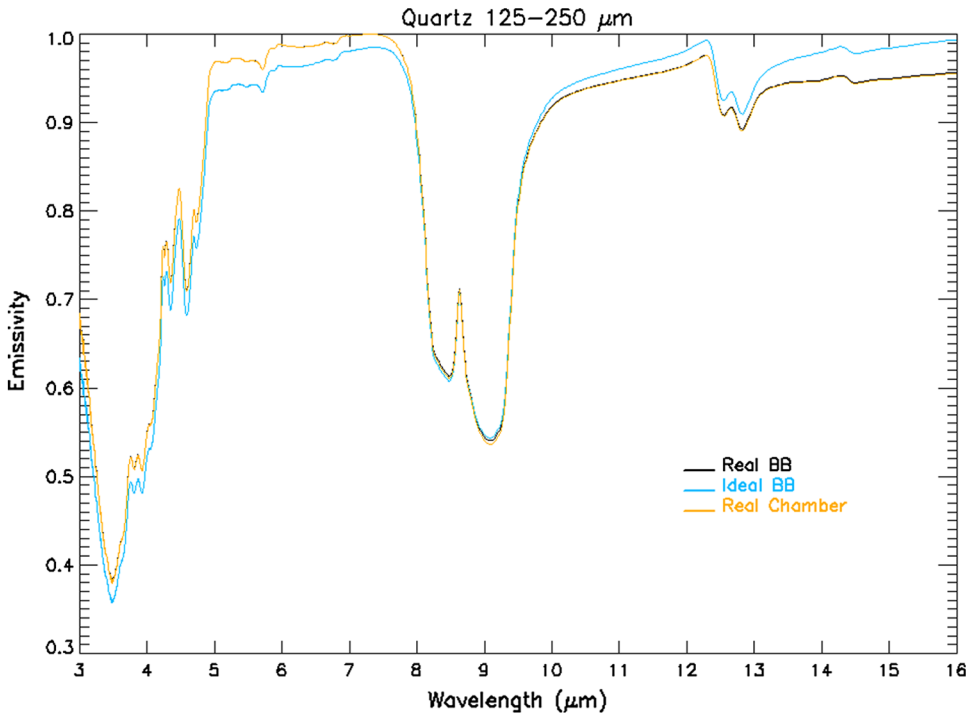

Fig. 2 Quartz 125- to 250-μm separately calibrated taking into account the real emissivity curve for the calibration blackbody (black curve), BB emissivity equals 1.0 along the whole wavelength range (light blue curve), and using the furnished emissivity curve for the black paint covering the emissivity chamber (orange dashed curve).

We also assumed a realistic emissivity for the paint of the chamber. However, the orange curve in Fig. 2 shows how little effect this setting has in comparison to assuming a constant unity emissivity for the chamber walls.

4 Characterizing the Instrumental Setup

The Bruker VERTEX 80v, which belongs to the latest generation of FTIR spectrometers, can be completely evacuated. The benefits of removing the air from the instrument are visible in Fig. 3 (upper panel), showing the same quartz samples measured having the instrument evacuated or purged (along three consecutive days).

Although the two curves are almost overlapping, the measurements under purged air (light blue data) show spectral signatures of water vapor and CO_2 in the recorded data, as can be seen in the lower panel of Fig. 3. The major CO_2 absorption band centered around 15 μm changes the shape of the continuum in the region between 14 and 16 μm, while the other main CO_2 band around 4.3 μm has a much more narrow influence area.

Water vapor has a series of small absorption bands between 5 and 8 μm, all of them clearly visible in the ratios. It is important to note that, since the sample temperature is estimated via the CF in the region between 6 and 11 μm, these small water bands influence its evaluation. This results in a slightly higher value for the sample temperature, resulting in a smaller derived emissivity. This difference is clearly visible around the Reststrahlen bands for most of the size separates, and in the region between 4.5 and 7 μm for all the samples.

With an additional hardware unit, we can use our VERTEX 80V instrument to measure transmission of filters or slabs of material. We took advantage of this utility to measure the transmission of our external windows, the KBr used with the MCT detector, and the CsI for the DTGS. There is a general concern, especially for CsI, that the expended exposure to the humidity in the air causes degradation. The measurement of the two kinds of materials used shows a very similar transmittance factor, and the comparison between used (almost 1000 h each window) and

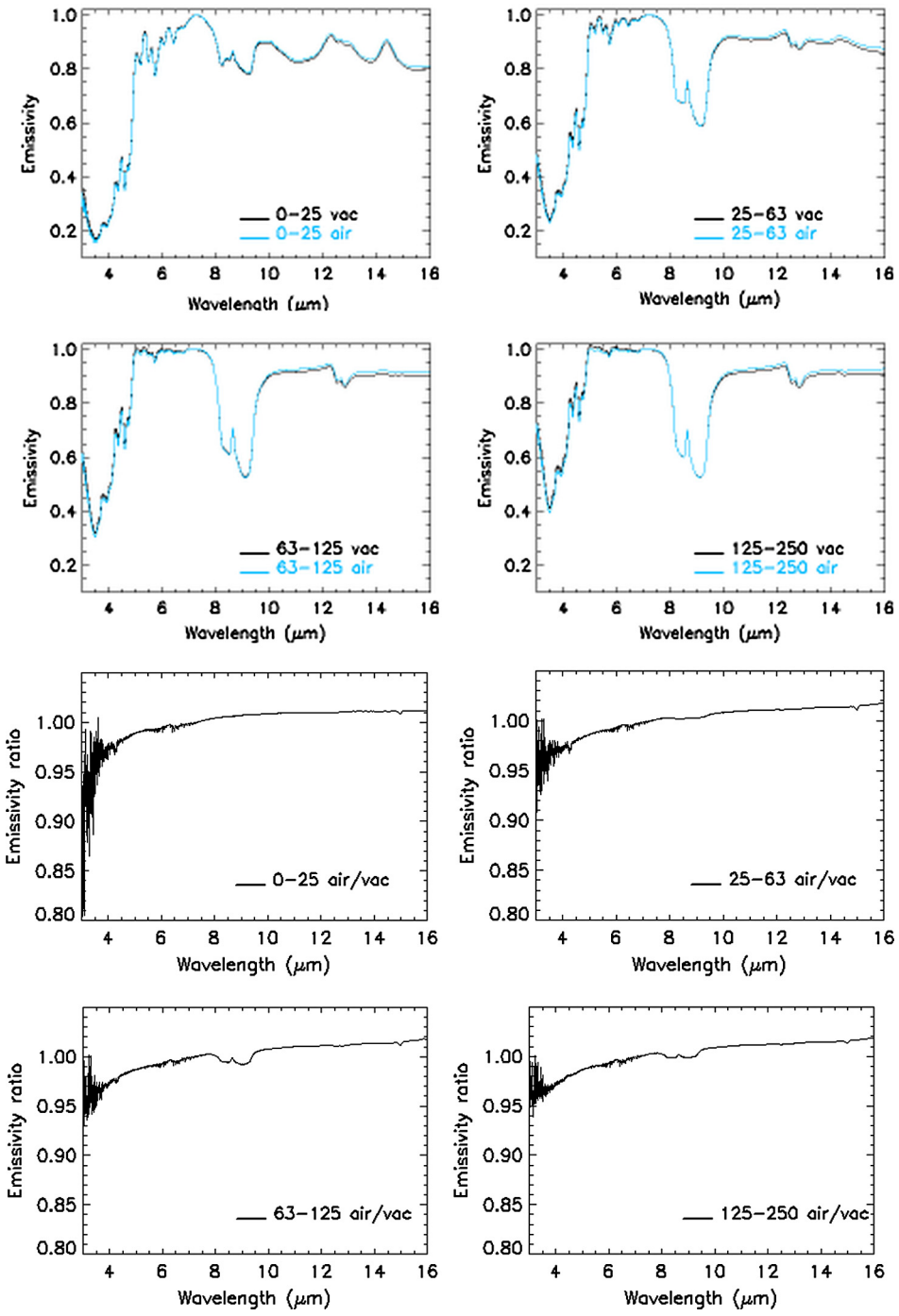

Fig. 3 Upper panel: emission spectra of the four BED typical grain size separates for quartz, measured with the instrument under vacuum (black curves) and under air purging (light blue curves). Lower panel: ratio between measurements taken with the spectrometer in air and in vacuum.

new windows let us conclude that the entrance windows did not degrade significantly (Fig. 4). Therefore, we exclude negative effect for the accuracy of our measurements.

5 Influence of Sample Preparation

The cups containing the four grain size separates to be measured are always prepared by following the same method: the particles are poured in the cup and then, using a thin metallic

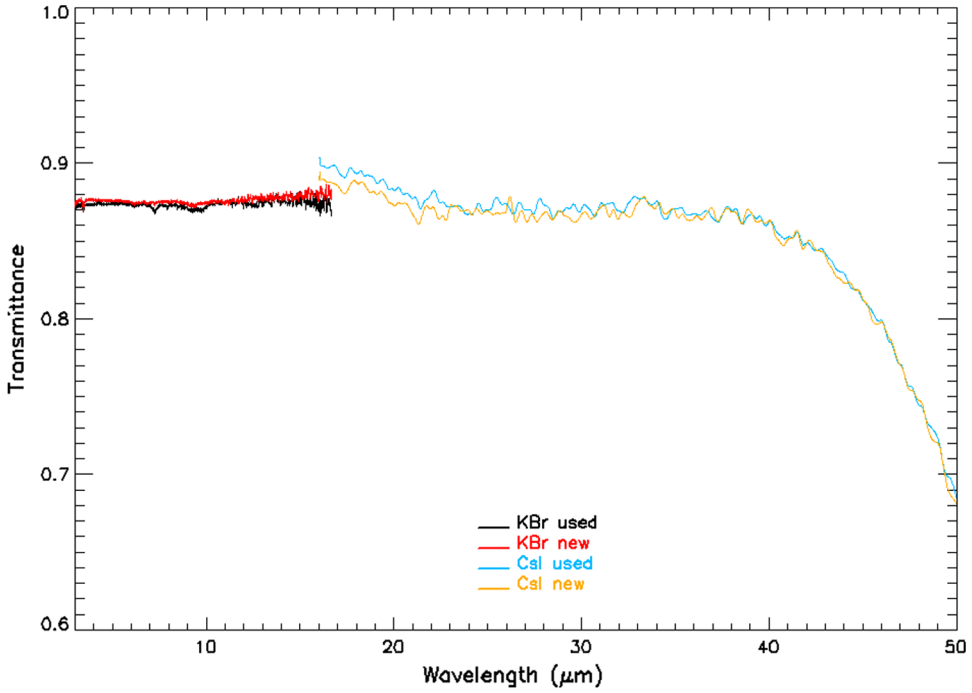

Fig. 4 Transmission spectra of the external ports used for the measurements with the two detector setups.

cylindrical bar, and the material in excess is gently removed to form a flat surface. The process is very carefully carried out to avoid pressing the material in the cup, which could lead to an alteration of the measured data. The flat surface procedure has been chosen because it is most similar to the one occurring for the calibration measurements, when an almost perfect flat blackbody surface is measured.

To test the influence of the surface orientation on the measured data, we filled five equal cups with quartz powder in the 45- to 63-μm grain size range, shaping the content as flat, concave,

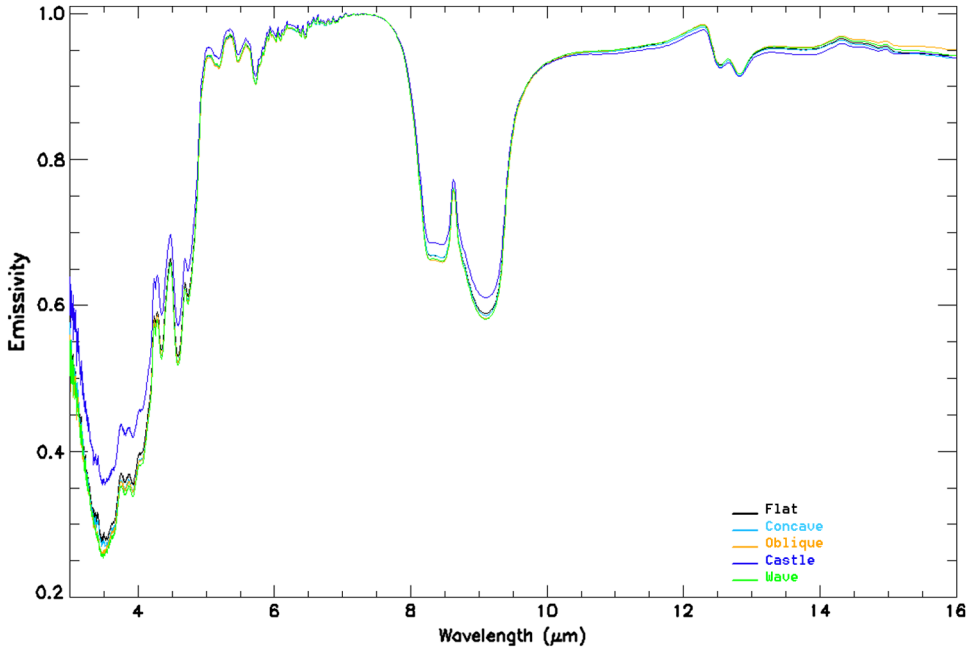

Fig. 5 Emission spectra of five different cups of quartz, in the 45- to 63-μm grain sizes range. The surfaces have been differently molded to study the effect of the surface shape on the measured data.

oblique, castle (obtained by depositing the grains in the cup without pressing or shaping them, so to have a low bearing strength among them), and wavy (simulating a sand dune-like scenario); the measurements are shown in Fig. 5.

It is interesting how the differences between the five cups are very limited in the region between 5 and 8 μm and in the region between 10 and 16 μm. The most significant changes appear around the two larger absorption features, in the region between 8 and 10 μm (the Reststrahlen band) and in the 3- to 5-μm region. Our device is calibrated to give the best results for an emitting planar surface, placed at a fixed distance from the parabolic mirror. Some of the differences seen in the five surfaces' data could be explained by the nonplanarity of some of the surfaces, where a certain amount of the normal emitted energy is not captured from the mirror. The same effect is found when analyzing remote sensing data coming from a planetary surface that have to be corrected for the emission angle, that is, the angle between the instrument line of sight and the normal to the observed surface.[5] The measurements highlight the necessity for a careful and repeatable procedure for sample preparation.

It is a well-known phenomenon that when crushing the minerals to obtain the desired grain sizes, many small particles having diameter size of few microns remain attached to the larger ones, and that these fine particles influence the measured spectra.[10] To quantify this effect on our measurements, we dry-sieved quartz in the typical BED four grain size fractions and successively a portion of each fraction was wet sieved, using distilled water, to remove the attached fine particles. Even the 0- to 25-μm fraction was filtrated with distilled water to partially remove some of the smaller particles (grains smaller than 5 μm) that are most abundant in this grain size fraction.

The measured spectra are shown in Fig. 6, in black the dry sieved and in light blue the wet sieved. For the two larger fractions (shown in the lower part of Fig. 6), the effect of attached fine particles is relevant only in the Reststrahlen bands (the region between 7 and 10 μm), while for the other smaller particles (upper part of Fig. 6) the whole spectral region is affected. In the case of smaller particles, volume scattering dominates the spectra, thus changing the overall shape, position, and depth of the bands, while for larger particles the surface scattering still dominates; hence the spectra change significantly only in the Reststrahlen band region.[11]

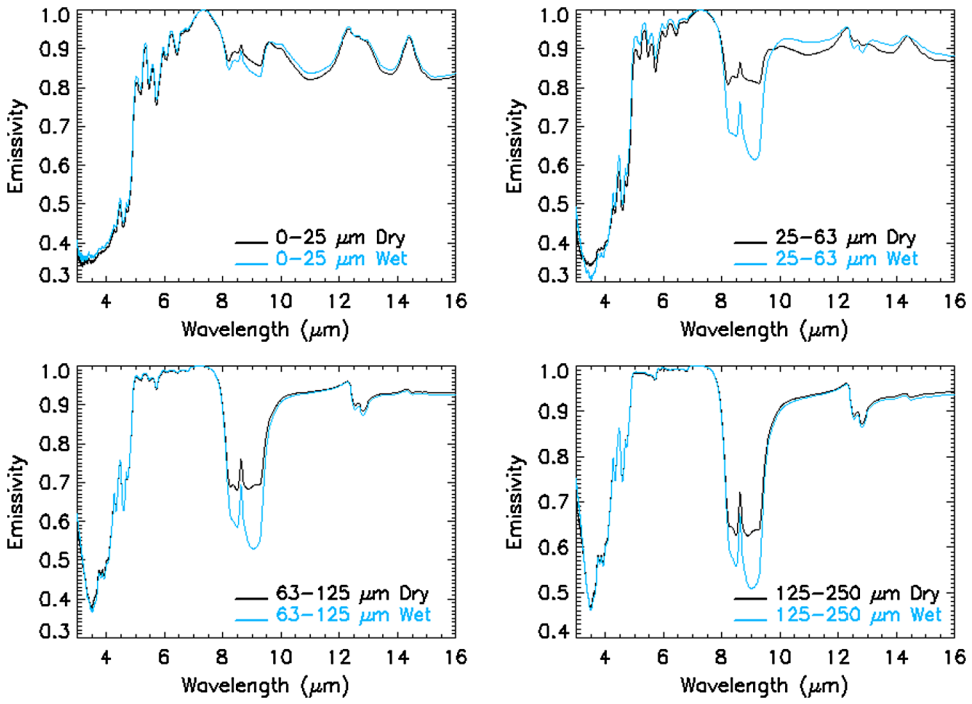

Fig. 6 Emission spectra of quartz typical BED grain size fractions, dry sieved (black) and wet sieved (light blue).

6 Estimation of Measurement Errors

By definition, the normal thermal emittance of an object is the ratio of the spectral radiance of a sample at a uniform temperature T, to that of an ideal (Planckian) blackbody at the same temperature, measured under identical conditions (of wavelength, direction, solid angle, polarization, etc.). This means that for minerals and rocks, their normal emissivity is the first-order temperature independent, at least for those temperatures lower than the one inducing a change in the crystal structure.

To verify this behavior in our setup, we measured BED quartz in the 125- to 250-μm grain size fractions, at four different heater temperatures (90°C, 120°C, 150°C, and 180°C). Each time the sample was put in the oven at the desired measurement temperature and, after reaching it, the sample was placed on the heater in the chamber for 30 min to reach equilibrium. Each measurement has been calibrated using the same algorithm. In Fig. 7, the differences between the spectrum taken at 180°C and the others are shown.

Sample temperature can be derived from calibrated sample radiance (B_{samp}). Under the assumption that $R_{\text{samp}} = 1 - \varepsilon_{\text{samp}}$, we can write the sample emissivity Eq. (1) in the following way:[8]

$$\varepsilon_{\text{samp}} B_{\text{samp}} + R_{\text{samp}} \varepsilon_{\text{env}} B_{\text{env}} = \frac{I_{\text{samp}}}{F} + \varepsilon_{\text{inst}} B_{\text{inst}}. \tag{3}$$

If we assume that the Christiansen feature (or frequency, CF) occurs at that frequency where the material's refractive index approach the refractive index of the medium, this results in a minimum in backscattering and also a minimum in reflectance or a maximum in emittance. Assuming $\varepsilon_{\text{samp}}$ equals 1 (close to be true for most of silicate minerals[7]), we can rewrite Eq. (3) as[8]

$$B_{\text{samp(CF)}} = I_{\text{samp(CF)}}/F + \varepsilon_{\text{inst}} B_{\text{inst(CF)}}, \tag{4}$$

where CF stands for the unique Christiansen frequency. Inverting the Planck function, we can compute the brightness temperature of the sample, derive the brightness temperature for all the wavelengths of the spectrum, and then use the maximum temperature as sample temperature.[8]

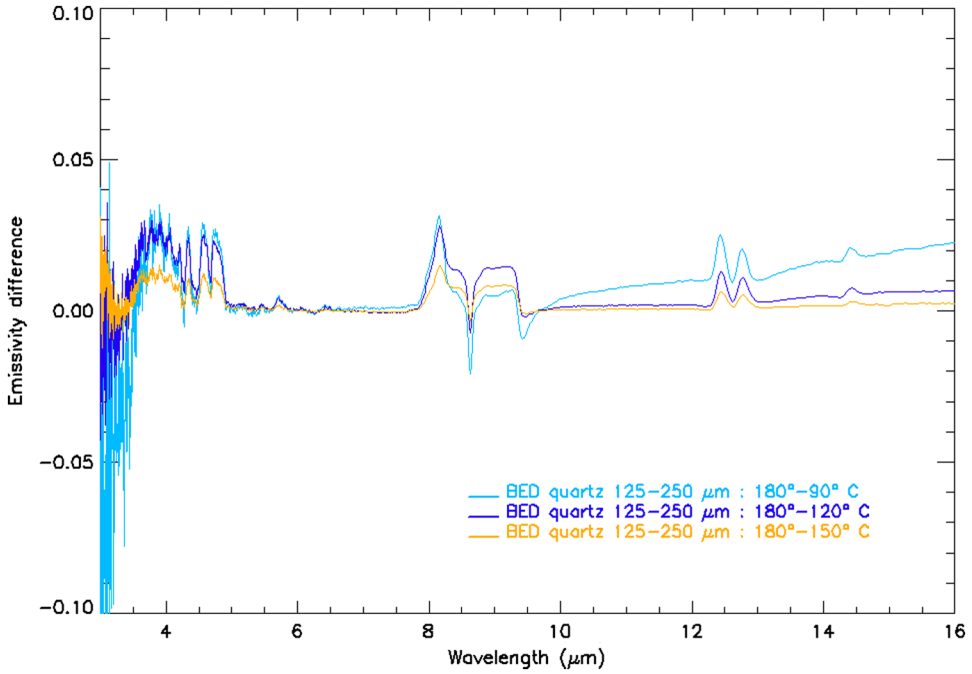

Fig. 7 Difference of emission spectra of BED quartz larger grain size fraction, measured at four different temperatures.

The difference between the measurements taken at four temperatures never exceeds 2% of the measured signal. It has to be taken into account that increasing the sample temperature increases the SNR. This could partly explain the small variations seen in the spectra in the region lower than 5 μm, where the measured signal is very low in any case.

The two principal sources of errors in our emissivity measurements are the instrument or the operator. Instrument includes here the whole setup of spectrometer + sample chamber. Instability in the temperature of each component, of the sample heater, or in the detector performances may lead to measurement errors. On the other hand, since our instrument field of view is 48 mm, while each sample cup is 50 mm in diameter, an inaccurate positioning of the cup on the heater (lying under the parabolic mirror) is another source of errors, attributed to the operator. The same is true for an inhomogeneous procedure in the sample cup preparation.

To test the instrument stability (repeatability of the measurements), we prepared a cup containing BED quartz with grain dimensions between 125 and 250 μm. After being heated in the oven, the cup was put on the heater at 180°C. Our standard procedure was to wait 30 min before measurement, to have time for the sample temperature to stabilize and for the air-purging system to clean the air from moisture and CO_2 that entered into the chamber when changing the sample. Then, a series of 11 measurements have been taken, each 5 min after the other. Figure 8 shows all the 11 measurements in the whole spectral range (MCT+DTGS detectors) (each spectrum is plotted with a different color), and their average. The picture proves how stable the system of instrument-detector-sample chamber environment is, since no difference is noticeable during 1 hour of data acquisition. This means that the instruments (and the detectors) are highly constant over time, the sample chamber maintains its constant temperature, and the sample heater delivers a very stable energy to the sample cup, keeping it at a constant temperature.

The deviation (Fig. 9) remains well below 0.2% in the whole spectral range, and below 0.1% for most of wavelengths larger than 4 μm. The increase for wavelengths shorter than 4 μm is due to the increasing noise in that region.

The last test of the set was defined to quantify the error in the sample preparation, and positioning on the heater, all of them depending on the precision of the operator (reproducibility). Three identical cups containing the same quartz 125- to 250-μm fraction were prepared, heated in the oven and then on the heater at 180°C, to be measured after 30 min of stabilization time. The

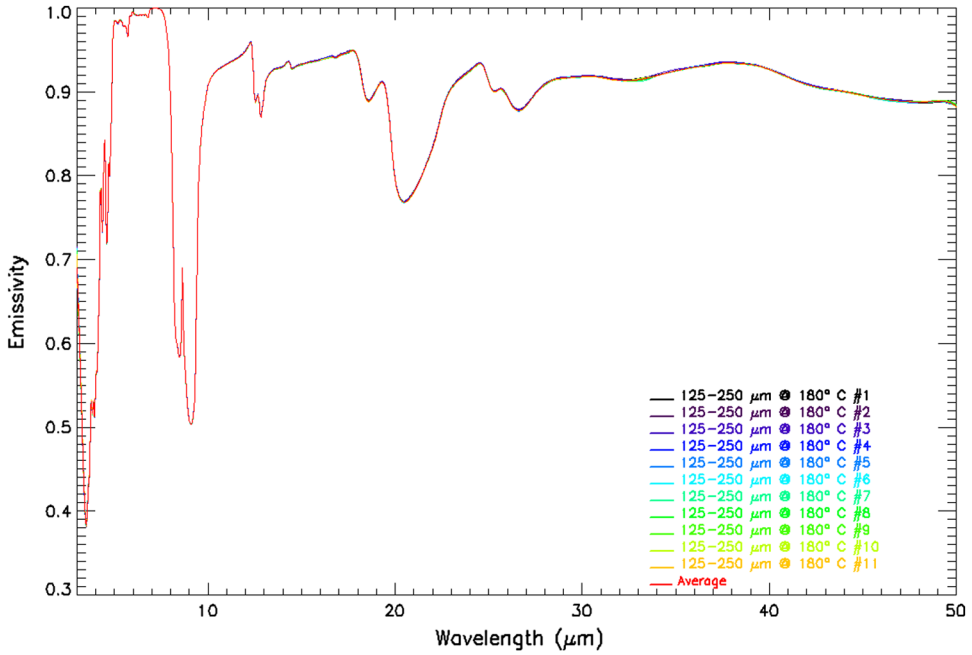

Fig. 8 Repeated measurements of BED quartz larger grain size fraction and average. The high stability of our setup is well described by Fig. 9, where the standard deviation (expressed in %) of the previous measurements is shown.

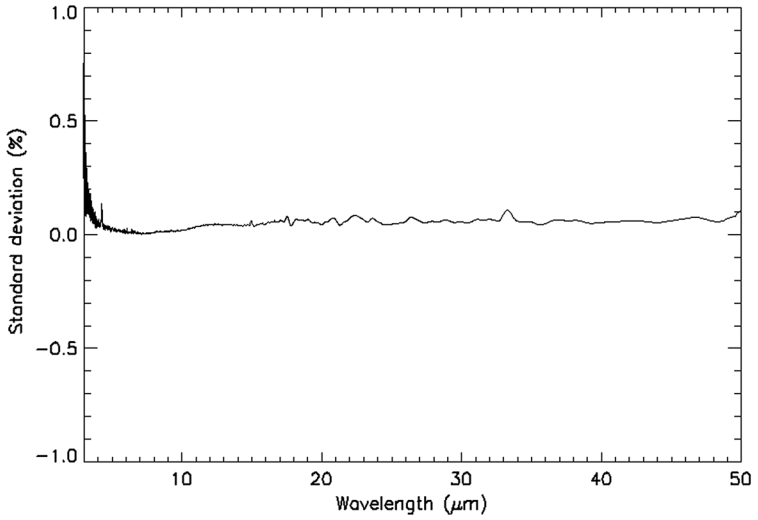

Fig. 9 Standard deviation (expressed in %) for the repeatability test of Fig. 8.

calibrated data for these three measurements are shown in Fig. 10 with the numbers 1, 2, and 3. The same cup 3 was, after measurements, taken out of the chamber and then immediately replaced on the heater, to reproduce a possible positioning error. This procedure was repeated two times, to give the measurements with indices 4 and 5 in Fig. 10. This plot proves how little are the errors that can derive from the sample preparation (we prepared three different cups of the same material) and positioning. In fact, from Fig. 11, in which the standard deviation relative to these measurements is shown, one can affirm that reproducibility error is always smaller than 0.3%, except for the region of increasing noise for wavelengths lower than 4 μm.

Again, a trend of the standard deviation with the emissivity is observed. If we sum the repeatability and reproducibility errors that we estimated, we get the picture shown in Fig. 12.

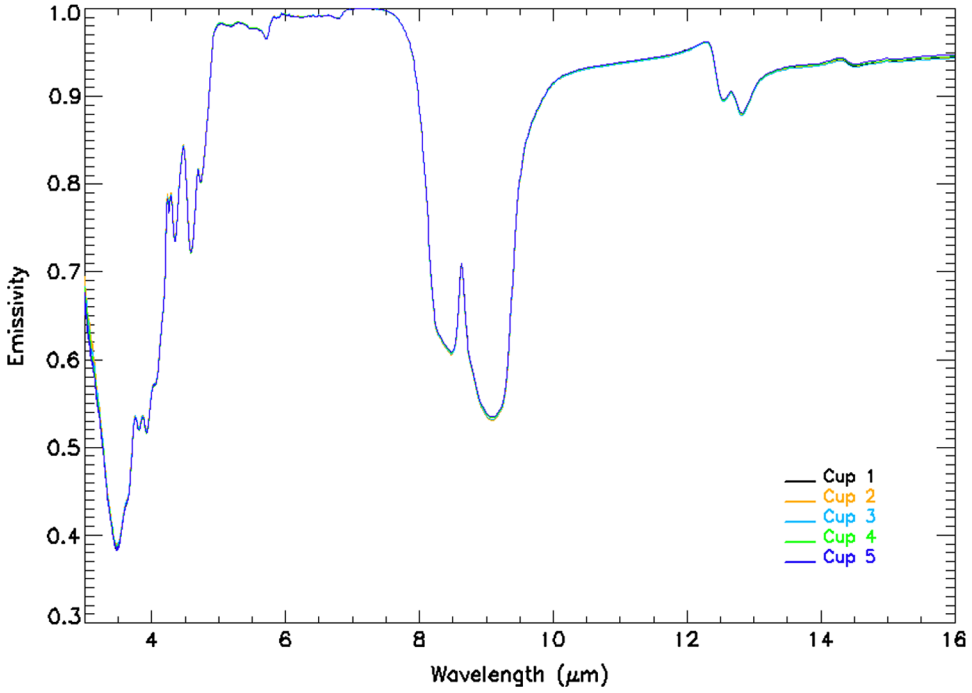

Fig. 10 Measurements of three cups containing the same quartz 125- to 250-μm samples (1 to 3) and cup 3 replaced two times on the heater (4 and 5).

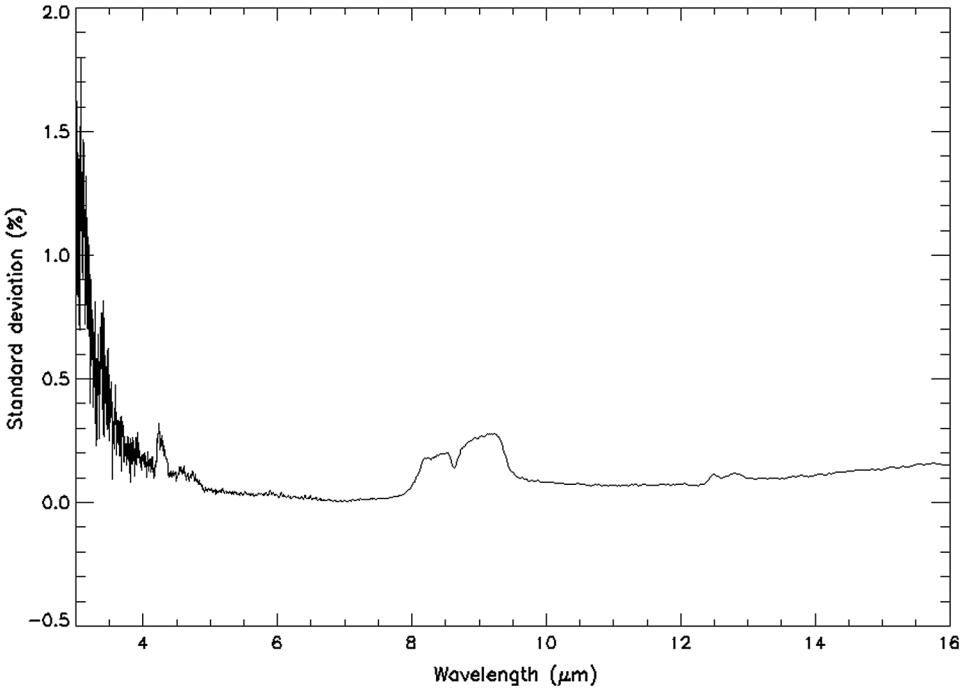

Fig. 11 Standard deviation (expressed in %) for the reproducibility test of Fig. 10.

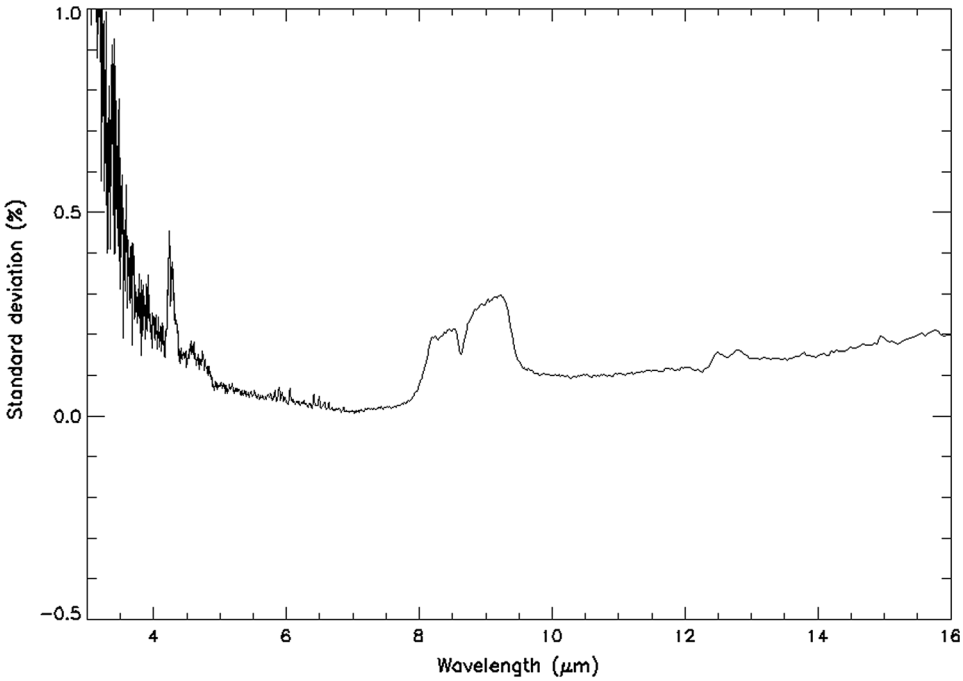

Fig. 12 Standard deviation for repeatability and reproducibility test of a BED emissivity measurement of quartz.

7 Summary and Conclusions

The performance of the setup for emissivity measurements in the planetary emissivity laboratory at DLR, Berlin, has been characterized via a series of tests. The calibration procedure has been optimized, checking which the more appropriate blackbody temperatures are, and improvements have been found when not considering the calibration blackbody ideal, but using its furnished

emissivity curve in the calibration algorithm. The benefits of evacuating the instrument have been demonstrated, so like the ones deriving from a flat surface preparation. Furthermore, the huge spectral effect of clinging fines on the measured samples has been shown. Instrument, detector, and external port stability were important checks, successfully passed by our equipment. From these tests, an instrumental error (expressed in % of the calibrated emissivity) has been derived. It was, moreover, not trivial to analyze the temperature independence of our results; from this we could conclude that our procedure for measuring and calibrating the data in the BED is correct. Errors deriving from sample preparation and target positioning (repeatability and reproducibility) have been characterized, and expressed in % of the calibrated value, so to be applied to all the entries of the BED library. In the future, these errors will be archived and distributed together with the calibrated data.

References

1. V. C. Farmer, *The Infrared Spectra of Minerals*, Mineral. Soc., London, UK (1974).
2. P. R. Christensen et al., "A thermal emission spectral library of rock-forming minerals," *J. Geophys. Res.* **105**(E4), 9735–9739 (2000), http://dx.doi.org/10.1029/1998JE000624.
3. P. R. Christensen and S. T. Harrison, "Thermal infrared emission spectroscopy of natural surfaces: application to desert varnish coating on rocks," *J. Geophys. Res.* **98**(B11), 19819–19834 (1993), http://dx.doi.org/10.1029/93JB00135.
4. V. E. Hamilton, "Thermal infrared emission spectroscopy of the pyroxene mineral series," *J. Geophys. Res.* **105**(E4), 9701–9716 (2000), http://dx.doi.org/10.1029/1999JE001112.
5. J. W. Salisbury et al., *Infrared (2.1–25 μm) Spectra of Minerals*, John Hopkins Univ. Press, Baltimore, Maryland (1991).
6. A. Maturilli, J. Helbert, and L. Moroz, "The Berlin emissivity database (BED)," *Planet. Space Sci.* **56**(3–4), 420–425 (2008), http://dx.doi.org/10.1016/j.pss.2007.11.015.
7. S. W. Ruff et al., "Quantitative thermal emission spectroscopy of minerals: a laboratory technique for measurement and calibration," *J. Geophys. Res.* **102**(B7), 14899–14913 (1997), http://dx.doi.org/10.1029/97JB00593.
8. A. Maturilli et al., "Emissivity measurements of analogue materials for the interpretation of data from PFS on mars express and MERTIS on Bepi-Colombo," *Planet. Space Sci.* **54**(11), 1057–1064 (2006), http://dx.doi.org/10.1016/j.pss.2005.12.021.
9. C. Monte et al., "Radiation thermometry and emissivity measurements under vacuum at the PTB," *Int. J. Thermophys.* **30**(1), 203–219 (2009), http://dx.doi.org/10.1007/s10765-008-0442-9.
10. J. W. Salisbury, A. Wald, and D. M. D'Aria, "Thermal-infrared remote sensing and Kirchoff's law, 1, laboratory measurements," *J. Geophys. Res.* **99**(B6), 11897–11911 (1994), http://dx.doi.org/10.1029/93JB03600.
11. J. W. Salisbury and A. Wald, "The role of volume scattering in reducing spectral contrast of reststrahlen bands in spectra of powdered minerals," *Icarus* **96**(1), 121–128 (1992), http://dx.doi.org/10.1016/0019-1035(92)90009-V.

Alessandro Maturilli is a postdoctoral researcher at the Institute of Planetary Research of the German Aerospace Center (DLR). He received his MS degree in mathematics from the University of Rome "La Sapienza" in 1998 and his PhD degree in aerospace engineering from the University of Naples "Federico II" in 2005. He is the author of more than 100 journal papers. His current research interests include visible to far-infrared spectroscopy, mineralogical composition of planetary surfaces, and emission spectroscopy. He is a member of SPIE.

Joern Helbert is a researcher at the Institute of Planetary Research of the German Aerospace Center (DLR). He received his MS degrees in physics at the Technical University of Braunschweig in 1997 and his doctorate at the Free University of Berlin in 2003. He is the co-PI of the MERTIS instrument on the ESA Bepicolombo mission to Mercury. His current research interests include visible to far-infrared spectroscopy, mineralogical composition of planetary surfaces, emission spectroscopy. He is a member of SPIE.